Inorganic Chemistry
Article

Inorg. Chem. **2011**, *50*, 1005–1013 **1005**
DOI: 10.1021/ic101679n

Structures of Vanadium(III)-Ethylenediamine-*N*,*N*′-diacetato-*N*,*N*′-di-3-propionato Complexes. Critical Role of p_π-d_π Donation in Determining the Coordination Number†

Roland Meier,*,‡ Steffi Mitzenheim,§ Hans Pritzkow,∥ and Rudi van Eldik‡

‡*Inorganic Chemistry, Department of Chemistry and Pharmacy, University of Erlangen-Nürnberg, Egerlandstrasse 1, 91058 Erlangen, Germany,* §*Institut für Anorganische Chemie, Universität Leipzig, Johannisallee, 04103 Leipzig, Germany, and* ∥*Anorganisch-Chemisches Institut, Im Neuenheimer Feld 270, 69120 Heidelberg, Germany*

Received August 18, 2010

Li[V(eddadp)]·3H_2O (**1a**) and Cs[V(eddadp)]·2H_2O (**1b**) were characterized by X-ray crystallography. **1a** crystallizes in the monoclinic space group *Cc* with *a* = 11.467(7) Å, *b* = 13.398(8) Å, *c* = 12.529(8) Å, β = 114.85(4)°; *V* = 1746.7(2) Å^3, and *Z* = 4; **1b** crystallizes in the monoclinic space group $P2_1/n$ with *a* = 10.265(5) Å, *b* = 11.673(6) Å, *c* = 15.507(8) Å, β = 104.29(2)°, *V* = 1800.6(2) Å^3, and *Z* = 4. The solution structure of **1** has been ascertained to be predominantly six-coordinated with a hexadentate eddadp which is based on a comparison of the electronic and Raman spectra of aqueous solutions of **1** with those in the solid state.

1. Introduction

The structural study of $[V(eddadp)]^-$ complexes was started as a part of our program to analyze the coordination chemical preference of V^{III} in various coordination spheres. We desired to elucidate the effects that change on going from six- to seven-coordination by studying the properties of the complexes in solution and the solid state.[1,2]

Various structures of V^{III} complexes with edta[3,4] and closely related ligands[5−8] were characterized by X-ray diffraction. In all these structures, seven-coordinate V^{III} centers were found, and the ligands formed five-membered chelate rings exclusively. As soon as ligands are bound to V^{III} where six membered rings are formed upon coordination (cf. Chart 1 for the composition of eddadp = ethylenediamine-*N*,*N*′-diacetate-*N*,*N*′-dipropionate),

Chart 1

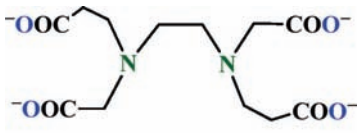

eddadp

the solid state complex seems to prefer six-coordination.[9,11] The complexes in which V^{III} has shown a CN (coordination number) of 6 included the salt K[V(eddadp)]·2H_2O (**1c**).[11] Six-membered rings were believed to hamper adoption of CN 7[2] because L−M−L′ bite angles in the range $< 76°$ (typical for V^{III} CN 7 complexes[5−8]) are difficult to be realized with six-membered chelate rings.

Because structures of eddadp complexes with 3d ions known so far showed six-coordination,[12−16] the finding of a CN 7 metal center in Na[Ti(eddadp)(H_2O)]·6H_2O[17] was a surprise. The occurrence of a seven-coordinate Ti^{III} center in $[Ti(eddadp)(H_2O)]^-$

† This paper is dedicated to the late Dr. Karlheinz Schmidt (DFG Bonn) for his engagement to support East German chemists in the application for research funding.

*To whom correspondence should be addressed. E-mail: roland.meier@chemie.uni-erlangen.de.

(1) Meier, R.; Boddin, M.; Mitzenheim, S. In *Bioinorganic Chemistry: Transitions Metals In Biology and their Coordination Chemistry*; VCH: Weinheim, Germany, 1997; Chapter A-7.
(2) (a) Meier, R.; Boddin, M.; Mitzenheim, S.; Schmid, V.; Schönherr, T. *J. Inorg. Biochem.* **1998**, *69*, 249. (b) Schönherr, T.; Schmid, V.; Meier, R. *Spectrochim. Acta* **1998**, *A54*, 1659.
(3) Shimoi, M.; Saito, Y.; Ogino, H. *Bull. Chem. Soc. Jpn.* **1991**, *64*, 2629.
(4) Miyoshi, K.; Wang, J.; Mizuta, T. *Inorg. Chim. Acta* **1995**, *228*, 165.
(5) Shepherd, R. E.; Hatfield, W. E.; Ghosh, D.; Stout, C. D.; Kristine, F. J.; Ruble, J. R. *J. Am. Chem. Soc.* **1981**, *103*, 5511.
(6) Ogino, H.; Shimoi, M.; Saito, Y. *Inorg. Chem.* **1989**, *28*, 3596.
(7) Shimoi, M.; Miyamoto, S.; Ogino, H. *Bull. Chem. Soc. Jpn.* **1991**, *64*, 2549.
(8) Okamoto, K.-I.; Hidaka, J.; Fukagawa, M.; Kanamori, K. *Acta Crystallogr.* **1992**, *C48*, 1025.
(9) Robles, J. C.; Matsuzaka, Y.; Inomata, S.; Shimoi, M.; Mori, W.; Ogino, H. *Inorg. Chem.* **1993**, *32*, 13.
(10) Kanamori, K.; Ino, K.; Maeda, H.; Miyazaki, K.; Fukagawa, M.; Kumada, J.; Eguchi, T.; Okamoto, K.-I. *Inorg. Chem.* **1994**, *33*, 5547.
(11) Kanamori, K.; Kumada, J.; Yamamoto, M.; Okayasu, T.; Okamoto, K.-i. *Bull. Chem. Soc. Jpn.* **1995**, *68*, 3445.
(12) Helm, F. T.; Watson, W. A.; Radanovic, D. J.; Douglas, B. E. *Inorg. Chem.* **1977**, *16*, 2351.
(13) Herak, R.; Manojlovic-Muir, L.; Djuran, M. I.; Radanovic, D. J. *J. Chem. Soc., Dalton Trans.* **1985**, 861.
(14) (a) Yamamoto, T.; Mikata, K.; Miyoshi, K.; Yoneda, H. *Inorg. Chim. Acta* **1988**, *150*, 237. (b) Meier, R.; Maigut, J.; Zahl, A.; Heinemann, F. W.; Buschmann, H. J.; van Eldik, R., manuscript in preparation.

Published on Web 12/29/2010

Chart 2

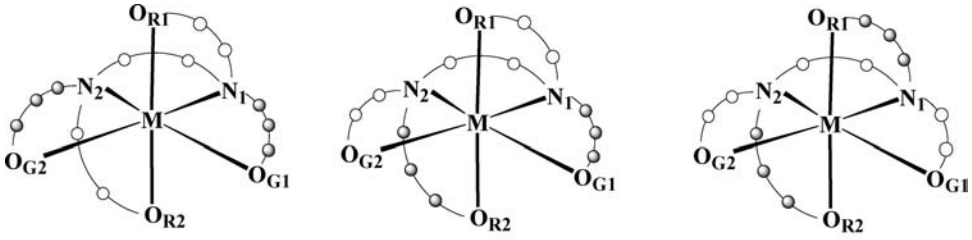

trans (O_5) *trans* (O_5O_6) *trans* (O_6)

was unexpected because K[V(eddadp)]·$2H_2O$[11] contains six coordinate V^{III}. It was therefore anticipated that salts of Ti^{III}-eddadp would also accommodate a six-coordinate metal center. In the case of edta, which can only form five-membered chelate rings, CN 7 complexes are found both for V^{III}[3,4] and Ti^{III}.[4,18,19] In the structure of Na[Ti(eddadp)-(H_2O)]·$6H_2O$, eddadp coordination takes place in the framework of the *trans*(O_6) geometrical isomer (cf. Chart 2; the coordinated water was omitted for the sake of comparison).

Six-coordinate structures gave rise to the *trans*(O_5) isomer (cf. Chart 2) exclusively.[12−16] In this isomer, the six-membered β-alaninato rings both coordinate in the octahedral plane, whereas the five-membered glycinato rings are directed out-of-plane. An X-ray structure of a *trans*(O_5O_6) V^{III} isomer is unknown to us, but this isomer was found in a related Cr^{III} complex during the chromatographic analysis of the reaction mixture.[20]

There are aminopolycarboxylato complexes where the CN in the solid state can obviously be triggered by the counter-cation, as found for the eight-coordinate salt [$Li(H_2O)_4$]-[Yb(heida)$_2$][21] and its CN 9 partner [$C(NH_2)_3$][Yb(heida)$_2$-(H_2O)]·$2H_2O$ (heida = *N*-Hydroxyethyl-iminodiacetate).[22] Likewise, the yellow six-coordinate Li[Fe(edta)]·$3H_2O$ and the dark-brown seven-coordinate Li[Fe(edta)(H_2O)]·$2H_2O$ complexes can be synthesized by selecting the proper reaction conditions.[23]

We decided therefore to characterize the lithium and cesium salts of $[V(eddadp)]^-$ by X-ray crystallography with the goal to try to isolate a CN 7 species of the type [V(eddadp)-(H_2O)]$^-$. Li^+ was selected as a counterion because of its strong preference for binding of crystal water molecules and the restricted tendency for interactions with carboxylato oxygens which was noted in related structural studies of various V(III) aminopolycarboxylato complex salts.[1,23,24] The opposite seems to be valid for larger alkali cations. Thus, Cs^+ was chosen to test conditions where the interactions with the carboxylato oxygens of the $[V(eddadp)]^-$ anion are preferred. Details in terms of the V^{III}-eddadp solution structure were expected from Raman- and VIS/NIR-spectral measurements.

2. Experimental Section

H_4eddadp (Sigma) and VCl_3 (Riedel de Haen) were used as received.

2.1. Spectral Measurements. UV/vis/NIR-spectra of solid samples and of complex solutions at constant pH values were recorded on a Perkin-Elmer Lambda-900 spectrophotometer. Transmission spectra of aqueous solutions containing V^{III}-eddadp complexes were recorded using Hellma QX 10 mm cuvettes (SUPRASIL 300). Baselines were recorded with identical cuvettes containing the pure solvent in both reference and sample beam. The solid samples were dissolved in doubly distilled water which was degassed by bubbling Ar and thermostatted at 25 °C.

Reflection spectra were measured using a small spot praying mantis accessory belonging to the Lambda-900. Sample holders with varying surface areas were used. Baselines were recorded using a white standard sample holder (PTFE-coated).

Raman spectra of solid samples were recorded with a BRUKER IFS 66 device, while spectra of complexes in aqueous solutions were measured with a JOBIN YVON Ramanor HG 2S. In both cases, the 457.9 nm line of an argon laser was applied as an excitation source.

2.2. Preparation of Li[V(eddadp)]·$3H_2O$ (1a). Under a nitrogen atmosphere, 0.01 mol (3.2 g) of H_4eddadp are suspended in 20 mL of H_2O with stirring. This is followed by addition of 0.01 mol (0.74 g) Li_2CO_3. After the development of CO_2 has ceased, 0.01 mol (1.57 g) VCl_3 are poured to this solution. After a short period of stirring, the solution has a dark green color. Now, another 0.01 mol (0.74 g) Li_2CO_3 are added, and the stirring is continued. The solution pH is now at 6−7. The volume of the solution was reduced to 5 mL on a vacuum evaporator, and the deep greenish oil that had been formed was separated. The oil was layered with an equivalent volume of well degassed ethanol and stored in a well sealed flask at 5 °C in a refrigerator over 3 days. After this time, dark-green needle-like crystals are formed. These are removed by filtration, washed with ethanol and ether, and air-dried. Yield 3.0 g (70%). Anal. Calcd for $C_{12}H_{22}N_2LiO_{11}V$ (428.2): C, 33.7; H, 6.5; N, 5.2. Found: C, 34.0; H, 6.2; N, 5.0%.

Single crystals for X-ray diffraction measurements were prepared by layering a concentrated aqueous solution of **1a** in a test tube with a 4-fold volume of a 1:1 mixture of well degassed ethanol and methanol. After 2 days, crystals suitable for X-ray diffraction are separated at the boundary between the aqueous and alcohol phases.

2.2. Preparation of Cs[V(eddadp)]·$2H_2O$ (1b). This complex was prepared in the same way as described above for **1a** except that two portions of Cs_2CO_3 (0.01 mol; 3.3 g) were used to neutralize the protons released during complex formation. Eventually, dark green crystals resulted which were suitable for characterization by X-ray structure analysis.

(15) (a) Chuklanova, E. B.; Polynova, T. N.; Porai-Koshits, M. A.; Poznyak, A. L. *Koord. Khim.* **1988**, *14*, 1115. (b) Mizuta, T.; Yamamoto, T.; Shibata, N.; Miyoshi, K. *Inorg. Chim. Acta* **1990**, *169*, 257. (c) Antsyshkina, A. S.; Sadikov, G. G.; Shkol'nikova, L. M.; Poznyak, A. L.; Sergienko, V. S. *Zh. Neorg. Khim.* **1996**, *41*, 1463.
(16) Radanovic, D. R.; Ianelli, S.; Pelosi, G.; Matovic, Z. D.; Tasic-Stojanovic, S.; Douglas, B. E. *Inorg. Chim. Acta* **1998**, *278*, 66.
(17) Miyoshi, K.; Wang, J.; Mizuta, T. *Chem. Lett.* **1995**, 721.
(18) Mizuta, T.; Wang, J.; Miyoshi, K. *Bull. Chem. Soc. Jpn.* **1993**, *66*, 3662.
(19) Mizuta, T.; Wang, J.; Miyoshi, K. *Inorg. Chim. Acta* **1993**, *203*, 249.
(20) Kaizaki, S.; Byakuno, M.; Hayashi, M.; Legg, J. I.; Umakoshi, K.; Ooi, S. *Inorg. Chem.* **1987**, *26*, 2395.
(21) Polyakova, I. N.; Polynova, T. N.; Porai-Koshits, M. A. *Koord. Khim.* **1983**, *9*, 1563.
(22) Polyakova, I. N.; Senina, T. A.; Polynova, T. N.; Porai-Koshits, M. A. *Koord. Khim.* **1983**, *9*, 1131.
(23) Meier, R., Boddin, M.; Zahn, G.; van Eldik, R., manuscript in preparation.
(24) Meier, R.; Zahn, G., manuscript in preparation.

Table 1. Crystal Data and Details of the Structure Determinations for Li[V(eddadp)]·3H_2O (**1a**) and Cs[V(eddadp)]·2H_2O (**1b**)

	1a	**1b**
formula	C_{12} H_{22} Li N_2 O_{11} V	C_{12} H_{20} Cs N_2 O_{10} V
formula weight	428.20	536.15
crystal color, form	green, needle	dark green, block
crystal system	monoclinic	monoclinic
space group	*Cc* (No. 9)	$P2_1/n$ (No. 14)
Z	4	4
a [Å]	11.467(7)	10.265(5)
b [Å]	13.398(8)	11.673(6)
c [Å]	12.529(8)	15.507(8)
α [deg]	90.00	90.00
β [deg]	114.85(4)	104.29(2)
γ [deg]	90.00	90.00
V [A^3]	1746.7(19)	1800.6(16)
d_{calc} [g cm^{-3}]	1.628	1.978
crystal dimensions [mm]	0.20 × 0.25 × 0.60	0.30 × 0.40 × 0.40
T_{meas} [K]	203(2)	203(2)
diffractometer	Siemens-Stoe AED2	Siemens-Stoe AED2
absorption coefficient, *μ*, (mm^{-1})	0.630	2.598
μ(Mo*K*α) [mm^{-1}]	0.71070	0.71070
θ-range [deg]	2.48−30.00	2.16−30.00
no. refl. coll.	2894	5262
no. refl. unique	2894	5262
no. refl. obs. [$F_o > 4\sigma(F)$]	2720	4567
no. refined parameters (*p*)	266	315
R_1[a]	0.0265	0.0398
wR_2[b]	0.0617	0.0976
goodness-of-fit on F^2	1.03	1.04

[a] $R_1 = \sum||F_o| - |F_c||/\sum|F_o|$. [b] $wR_2 = [\sum w(F_o^2 - F_c^2)^2]/\sum(F_o)^2]^{1/2}$; $w = 1/[\sigma^2(F_o^2) + (0.0283P)^2 + 0.8476P]$ (**1a**) and $w = 1/[\sigma^2(F_o^2) + (0.0379P)^2 + 5.4857P]$ (**1b**), where $P = (F_o^2 + 2F_c^2)/3$.

Yield 3.0 g (56%). Anal. Calcd for $C_{12}H_{20}N_2CsO_{10}V$ (536.2): C, 26.9; H, 3.8; N, 5.3. Found: C, 26.6; H, 3.6; N, 5.2%.

2.3. Crystal structure determinations of 1a and 1b. Single crystals were prepared as described above. Crystal data and experimental details are compiled in Table 1. Intensity data were collected at −70 °C on a Siemens-Stoe AED2 diffractometer (Mo Kα radiation, $\lambda = 0.71073$ Å, graphite monochromator, *ω*-scans) up to $\Theta_{max} = 30°$. An empirical absorption correction was applied (*ψ*-scans). The structures were solved by direct methods and refined by full matrix least-squares methods based on F^2 with all measured reflections. All non-hydrogen atoms (except Li^+) were given anisotropic temperature factors. In the case of **1b**, all hydrogen atoms were located in a difference Fourier map and refined isotropically. In the case of **1a**, only the water protons were located in a difference Fourier map, and the remaining protons were inserted into calculated positions. The calculations were performed using the Programs SHELXS-86 and SHELXL-97.[25] Crystallographic data (excluding structure factors) for the structures reported in this paper have been deposited with the Cambridge Crystallographic Data Center as supplementary publication nos. CCDC-179409 (**1a**) and CCDC-179410 (**1b**). Copies of the data can be obtained free of charge on application to CCDC, 12 Union Road, Cambridge CB2 1EZ, U.K. (fax: (+44)1223−336−033; e-mail: deposit@ccdc.cam.ac.uk).

3. Results

3.1. Structural Features of 1a and 1b. (a). V−L Bond Distances. The refinement data of the structure determinations of **1a** and **1b** are compared in Table 1. Selected bond distances and angles of **1a** and **1b** are summarized in Table 2. The structures of the complex anions in **1a** and **1b** are shown in the ORTEP plots of Figure 1. As found before for the potassium salt **1c**,[11] the geometrical isomer encountered in the complex anions of both **1a** and **1b** is of the *trans*-(O_5) type where both the five-membered rings coordinate out-of-plane (R rings) and both the six-membered rings coordinate in-plane (G rings, cf. Chart 2).

Table 2. Bond lengths [Å] and Angles [deg] Which Define the Coordination Environments in Li[V(eddadp)]·3H_2O (**1a**), Cs[V(eddadp)]·2H_2O (**1b**), and K[V(eddadp)]·2H_2O (**1c**)

	1a	**1b**	**1c**
V1−O1 $\mathbf{G_1}$	1.939(2)	1.940(2)	1.952(2)
V1−O5 $\mathbf{G_2}$	1.938(2)	1.979(3)	1.964(3)
V1−O3 $\mathbf{R_1}$	2.007(2)	1.980(3)	1.974(3)
V1−O7 $\mathbf{R_2}$	1.999(2)	1.983(3)	1.970(3)
V1−N1	2.169(2)	2.145(3)	2.149(3)
V1−N2	2.165(2)	2.156(3)	2.142(3)
O3−V1−O7	175.84(9)	166.7(1)	167.9(1)
O5−V1−N1	162.97(10)	168.2(1)	166.9(1)
O1−V1−N2	161.81(9)	170.4(1)	170.5(1)
O3−V1−N1	80.55(9)	80.3(1)	79.7(1)
O3−V1−O1	97.58(9)	98.8(1)	96.8(1)
O3−V1−O5	86.55(10)	88.1(1)	87.4(1)
O3−V1−N2	95.22(9)	88.9(1)	90.5(1)
N1−V1−N2	81.61(9)	85.5(1)	85.1(1)
N1−V1−O1	87.79(8)	90.0(1)	90.1(1)
N2−V1−O5	88.59(9)	92.4(1)	92.8(1)
O1−V1−O5	105.00(9)	93.7(1)	93.7(1)
O7−V1−N1	99.29(9)	91.9(1)	91.7(1)
O7−V1−O1	86.57(9)	91.9(1)	91.6(1)
O7−V1−O5	92.77(10)	99.1(1)	100.8(1)
O7−V1−N2	80.65(9)	79.8(1)	90.4(1)

1a crystallizes in the monoclinic space group *Cc* and seems to circumvent the orthorhombic space group $P2_12_12_1$ which was found in the isomorphous salts Li[M(eddadp)]·5H_2O

(25) (a) Sheldrick, G. M. *SHELXS86, Program for the Solution of Crystal Structures*; University of Göttingen: Göttingen, Germany, 1986. (b) Sheldrick, G. M. *SHELXL97, Program for Crystal Structure Determinations*; University of Göttingen, Göttingen, Germany, 1997.

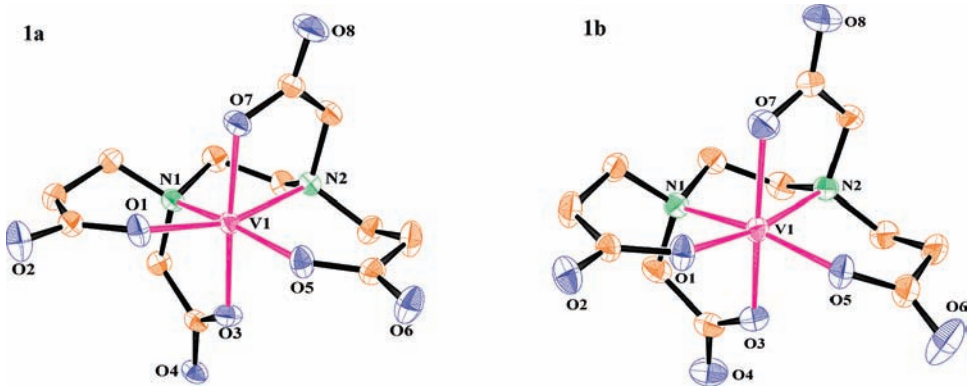

Figure 1. ORTEP drawings of the complex anions $[V(eddadp)]^-$ in the salts $Li[V(eddadp)]\cdot 3H_2O$ (**1a**) and $Cs[V(eddadp)]\cdot 2H_2O$ (**1b**). The Δ (ΔΛΔ) optical isomers have been refined in both cases. (All atoms are drawn at the 50% probability level).

with M = Cr^{III}[12] and Rh^{III}.[13] **1b** is isotypic to **1c** and the monoclinic space group $P2_1/n$ is encountered. The average V−O distance is very similar in the three salts (1.97 ± 0.04 Å in **1a**, 1.97 ± 0.02 Å in **1b** and 1.97 ± 0.02 Å in **1c**) and thus only slightly shorter than $V-O_{av}$ = 1.98 ± 0.03 Å in the related six coordinate V^{III} complex $Na[V(tmdta)]\cdot 3H_2O$ (tmdta = trimethylenediamine tetraacetate).[9] The mean V−N distance becomes shorter on going from **1a** ($V-N_{av}$ = 2.167(3) Å) via **1b** ($V-N_{av}$ = 2.151(8) Å) to **1c** ($V-N_{av}$ = 2.146(5) Å).

The individual V−O and V−N distances are quite different in **1a** and **1b**. This is obviously related to a varying influence of the counter cations (Li^+ vs Cs^+) and different packing effects in the crystals. The V−O distances in **1a** are quite uniform in terms of the individual $V-O_G$ and $V-O_R$ lengths. The former are both rather short (V1−O1 = 1.939(2) and V1−O5 = 1.938(2) Å) and virtually identical. These bonds are coupled to fairly obtuse (for $M-O_{carboxylato}$ bond in a β-alanine chelate ring) M−O−C angles ((C5−O1−V1) = 139.3(2)° and (C10−O5−V1) = 139.1(2)°). The length of the out-of-plane distances is V1−O3 = 2.007(2) and V1−O7 = 1.999(2) Å and coincides thus in the 3σ limit. Hence, $(V-O_R)_{av}$ is 0.065 Å longer than $(V-O_G)_{av}$.

In **1b**, only V1−O1 = 1.940(2) Å is in the range of the $V-O_G$ distances found in **1a** but V1−O5 = 1.979(3) Å is significantly longer (0.039 Å) than V1−O1. The $V-O_R$ distances in **1b** (V1−O3 = 1.980(3) and V1−O7 = 1.983(3) Å) are shorter by 0.022 Å than the analogous distances in **1a**. We assume that the influence of Cs^+ on the carboxylato oxygens is responsible for the variation of the V−L bond lengths between **1a** and **1b**. Details describing the Li−O and Cs−O bonding in the crystals of **1a** and **1b** will be presented in the next section.

Besides these distance variations, it has to be mentioned that also the $O_{R1}-V-O_{R2}$ angles differ drastically between **1a** (O3−V1−O7 = 175.84(9)°) and **1b** (O3−V1−O7 = 166.7(1)°). This difference is again related to the specifics of the Li−O and Cs−O interactions (cf. Supporting Information, Figure S1a and Figure S1b) in **1a** and **1b**, and details will be discussed below.

While the average V−O distance is about the same in **1a** and **1b**, subtle differences were noticed with the single V−O bond lengths. We relate the constancy of $(V-O)_{av}$ to a uniform capacity of a V^{III} center to accept charge density from the donor atoms. To elucidate the nature of the V−O and V−N interactions in a more detailed way, a comparison was made with bonds in related M^{III}-eddadp complexes. Such a comparison is most suitably done by means of a Shannon plot as shown in Figure 2. In a Shannon plot, the actual M−L distances from X-ray structures are related to hypothetical bond lengths derived from the sum of the Shannon radii (Shannon radius = IR)[35] between the appropriate metal ion M and the ligand donor atom L ($(M-L)_{Shannon} = \sum IR\ M^{n+} + IR\ L$). What results from this comparison is the difference $\Delta = \{(M-L)_{obs} - (M-L)_{Shannon}\}$ where $(M-L)_{Shannon}$ for $(V^{III}-N)$ = (0.64 + 1.46) = 2.10 Å and for $(V^{III}-O)$ = (0.64 + 1.35) = 1.99 Å. The Shannon parameters plotted in Figure 2 for the averaged M−L distances $(M-N)_{av}$, $(M-O)_{Gav}$, and $(M-O)_{Rav}$ concern those in the structures (from left to right) of $Li[Fe(eddadp)]\cdot 3H_2O$,[14b] **1a**, **1b**, and **1c**,[11] $Li[Cr(eddadp)]\cdot 5H_2O$,[12] $Ba[Ni(eddadp)]\cdot 6H_2O$,[16] $Ba[Co(eddadp)]\cdot 6H_2O\cdot ClO_4$,[15a] and $Li[Rh(eddadp)]\cdot 5H_2O$.[13] The Shannon parameter decreases if a M−L bond becomes shorter and vice versa.

What is seen in Figure 2 on going from left to right is a continuous decrease in the Shannon parameter for the M−N bonds, indicating a stepwise reduction of the M−N distances and thus an increasing affinity for bonding to nitrogen. The strongest M−N bonds are formed by the $4d^6$ ion Rh^{III} and the weakest by the $3d^5$ (high spin) Fe^{III} ion. In the latter case, the Fe−N bonds are presumably the longest because of the repulsions between the singly occupied $d_{x^2-y^2}$ orbital and the amine nitrogen lone pairs with σ symmetry. In the case of V^{III} as well as all the remaining M^{III} ions, the $d_{x^2-y^2}$ and d_{z^2} orbitals are not occupied with metal electrons. Thus, the M−N lengths are not only influenced by the affinity of the individual ions in forming M−N σ bonds, but the individual affinities for oxygen should also play a role here. If a metal ion's affinity for bonding with oxygen is larger than that for the metal−nitrogen interactions, the M−N bonds are elongated alongside the O−M−N *trans* interactions. Thus, one can conclude that the M−N bonds along a linear O−M−N arrangement become increasingly longer if the π donor strength of the oxygen donor atom increases. It follows for the bond lengths patterns in structures formed by the same ligand with different metal ions: The M−N bond is longest in the complex with the strongest π-accepting central ion during the M−O interaction. This was verified, for example, in complex structures with a

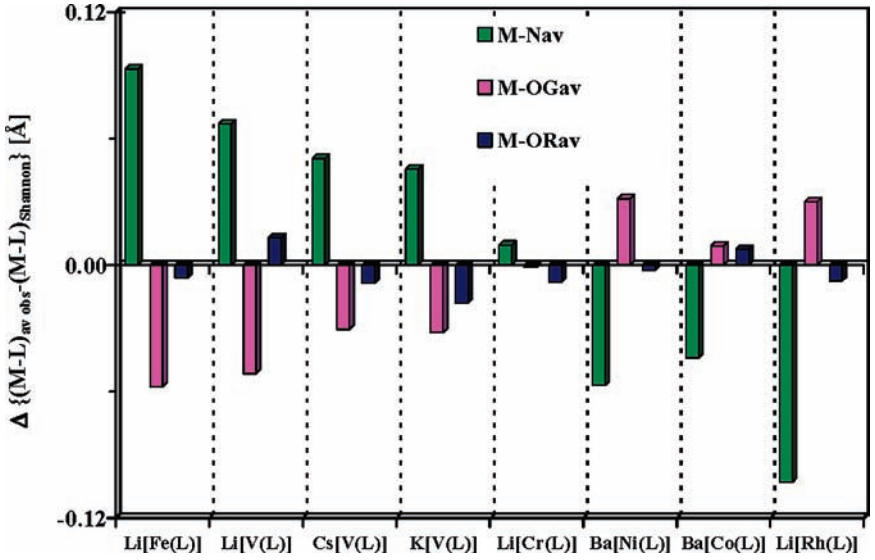

Figure 2. Shannon plot of the M−L distances in the complex anions of $[M^{III}(eddadp)]^-$ and $[M^{II}(eddadp)]^{2-}$ salt structures (L = $eddadp^{4-}$). Numbering of crystal water molecules has been omitted from the complex formulas.

triazacyclononane ligand containing three N-substituted phenolic rings.[26]

It was shown[27] that the π-accepting capacity of Cr^{III}, V^{III}, and Fe^{III} in their $[M(H_2O)_6]^{3+}$ ions increases in the order $d^3 < d^2 < d^5$ (hs). The increase in the Shannon parameter for the M−O_G bonds on going from Fe^{III} via V^{III} to Cr^{III} is in line with this finding. Furthermore, the constant increase of the Shannon parameter for the M−O_G bonds on going from left to right, reflecting a growth of the M−O distances, is both a consequence of the decreasing affinity for oxygen and of the increasing affinity for bonding to nitrogen. In the case of both the Co^{III} and the Rh^{III} complexes with their d^6 low spin electron configuration, the affinity for nitrogen is much larger than for oxygen because the three t_{2g} orbitals are double occupied. In this case, interactions with the carboxylato oxygen orbitals of π symmetry should result in antibonding repulsions.

In cases where M−N bonding is realized with empty e_g orbitals and M−O bonding is hindered by fully occupied t_{2g} orbitals, in-plane M−N attraction seems to be accompanied by M−O_G repulsion. Obviously as a consequence of this, the M−O_R bonds become shorter in these cases than the M−O_G bonds starting from Li[Cr(eddadp)]·$5H_2O$, and this relative shortening remains about the same in the Co^{III} and Rh^{III} structures.

The effects of the *trans*-interactions via the O_{G1}−M−N_2 and O_{G2}−M−N_1 arrangements have been visualized with averaged Shannon parameters in Figure 3. The more diffuse nature of the 4d- compared to 3d-orbitals in the case of the Rh^{III} structure leads obviously to a modified M−L bonding pattern of this $4d^6$ ion (cf. Figure 3). Thus, Rh^{III} was not considered in the linear regression plot of Figure 3. The remaining data give rise to a correlation coefficient of $R^2 = 0.96$.

(b). Differences in Packing Patterns between 1a and 1b. In the previous section, it was shown that subtle differences do exist between the individual M−L bonds in **1a** and **1b**. These variations originate from the different nature of both the counter cations Li^+ versus Cs^+. Details of the interactions between the complex anions and the counter cations and resulting packing pattern variations will be described below.

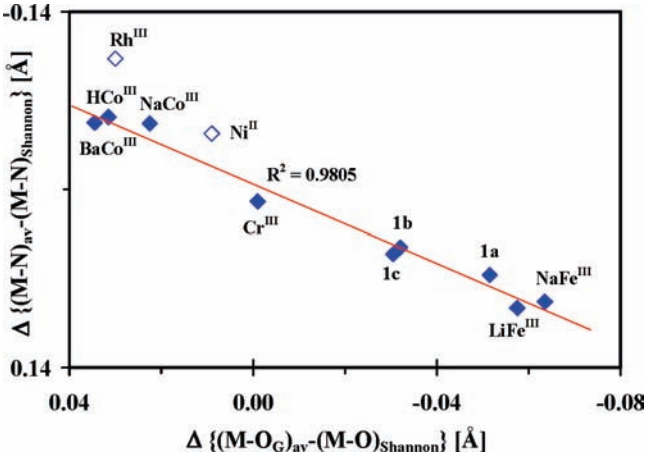

Figure 3. Linear dependence between averaged Shannon parameters of the $(M-N)_{av}$ and $(M-O_G)_{av}$ distances in structures of M^{III}-eddadp complexes as taken from Figure 2. The Rh^{III} and Ni^{II} structures have not been considered in the linear regression. (References: Cr^{III} = Li[Cr(eddadp)]·$5H_2O$,[12] Rh^{III} = Li[Rh(eddadp)]·$5H_2O$,[13] $BaCo^{III}$ = Ba[Co(eddadp)]·ClO_4·$6H_2O$,[15a] $NaCo^{III}$ = Na_3[Co(eddadp)]$_2$·ClO_4,[15b] HCo^{III} = [Co(Heddadp)]·$2H_2O$,[15c] Ni^{II} = Ba[Ni(eddadp)]·$6H_2O$,[16] **1a** and **1b** (this work), **1c**,[11] $NaFe^{III}$ = Na[Fe(eddadp)]·$5H_2O$[14a] and $LiFe^{III}$ = Li[Fe(eddadp)]·$3H_2O$ [14b]).

In **1a**, the $[V(eddadp)]^-$ units are arranged in such a way that the O_{R1}−V−O_{R2} axis (= O3−V1−O7; perpendicular to the pseudo C_2 axis through the complex molecule) of the complex molecule is roughly parallel to the cell vector ***a***. Li^+ coordinates two crystal water molecules and bounds to the uncoordinated oxygens O6 an O4 of neighboring eddadp complex anions. Thus, individual complex anions in the chains are linked via O6−Li−O4′ and O6′−Li-O4 connections as shown in Figure 4 (see also Supporting Information, Figure S1a). This bridging is part of infinite $[\{Li(OH_2)\}[V(eddadp)]_n$ chains which

(26) Auerbach, U.; Weyhermüller, T.; Wieghardt, K.; Nuber, B.; Bill, E.; Butzlaff, C.; Trautwein, A. X. *Inorg. Chem.* **1993**, *32*, 508.
(27) Kallies, B.; Meier, R. *Inorg. Chem.* **2001**, *40*, 3101.

extend in **1a** along the diagonal through the 010 (*ac*) plane. The intrachain V−O−V′ distance is 7.562 Å and the V−V′−V″ angle is 117.81°. Adjacent complex anions in the chain are related to each other by a glide plane such that the $[V(eddadp)]^-$ anions bridged by a single Li^+ ion differ in their overall chirality (cf. Figure 4). Interchain connection is realized by hydrogen bonds. One such bond is shown as dotted line in Figure 4 (O10−H101···O8, No. **6** in Supporting Information, Table S1). From Supporting Information, Table S1, where the bonding details of the H-bond network in **1a** are collected, it can bee seen that the third crystal water molecule O11 (not shown in Figure 4), which is not bound to Li^+, is involved in this interchain bridging by forming two hydrogen bonds along *a* (O9−H91···O11 (***4***) and O11−H112···O4 (***5***)) and one such bond along *b* (O11−H111···O2 (***2***)).

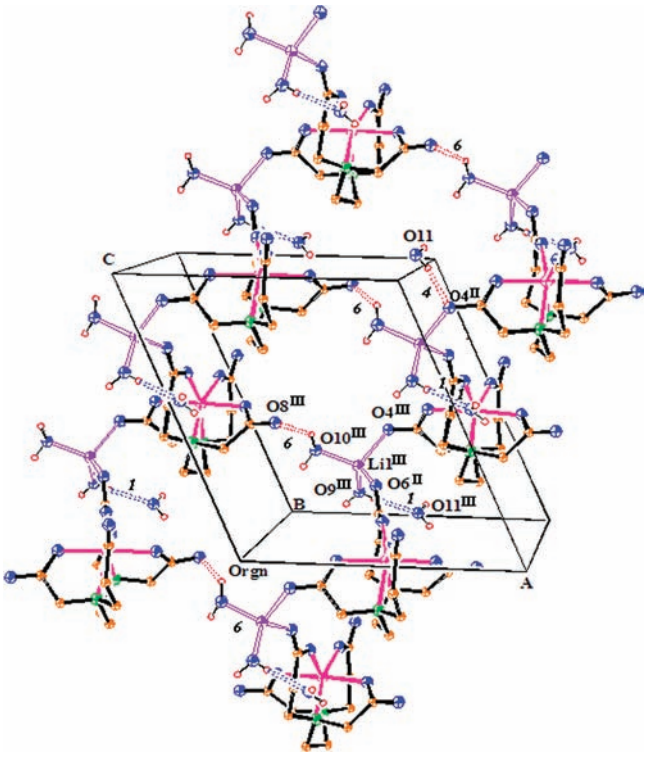

Figure 4. View onto the infinite $[\{Li(OH_2)\}[V(eddadp)]_n$ chains in the crystal structure of **1a**. Hydrogen bonds (dotted lines) are numbered as given in Supporting Information, Table S1a (Symmetry operations: $^{II} = x, -y + 1/2, -z + 1/2$; $^{III} = x + 1/2, y + 1/2, z$; $^{IV} = x + 1/2, -y + 1/2, z + 1/2$).

The mode of Li−O bonding and the network of hydrogens formed by crystal water molecules bound to Li^+ differ significantly to the analogous interactions in $Li[Cr(eddadp)]\cdot 5H_2O$[12] and $Li[Rh(eddadp)]\cdot 5H_2O$.[13] Both the latter structures are isomorphous to each other and crystallize in the orthorhombic space group $P2_12_12_1$. In contrast to **1a**, the Li−O tetrahedra are comprised by three crystal water molecules and only one uncoordinated carboxylato oxygen of eddadp. Thus Li^+ bridging of $[M(eddadp]^-$ units as found in **1a** does not take place in these salts. Instead, the protons at the Li-bound crystal water molecules are involved in strong hydrogen bonds that connect the homochiral $[M(eddadp]^-$ complex anions within the chains along the three 2_1 screw axes.[12,13]

In the crystals of **1b**, the $O_{R1}-V-O_{R2}$ axis (= O3−V1−O7) of $[V(eddadp)]^-$ is parallel to vector ***c***. The Cs^+ ion adopts CN 8 (with Cs−O lengths ranging from 3.006(3) for Cs−O2 and 3.409(4) Å for Cs−O8) (cf. Supporting Information, Table S2). It is bound to seven carbxylato oxygens from four adjacent $[V(eddadp)]^-$ ions and one crystal water molecule (cf. Figure 5 and Supporting Information, Figure S1b). The remaining crystal water molecule is involved in short hydrogen bonds (for details see Supporting Information, Table S1 and Figure S1b). On the basis of the Cs−O interactions with the carboxylato oxygens, a three-dimensional network of $[V(eddadp)]^-$ units is formed. The most remarkable feature is the bonding of Cs^+ with the three oxygens (O1, O5, and O3) that coordinate to the V^{III} center at the same time.

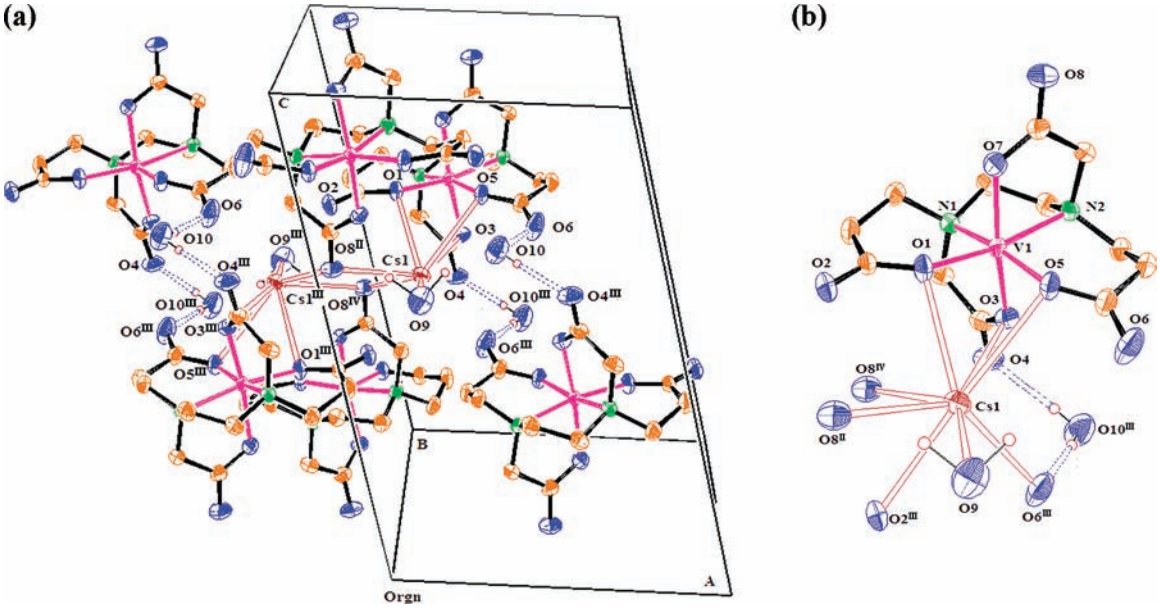

Figure 5. (a) Cs−O bonding in **1b**. Cs^+ has CN 8 and connects four $[V(eddadp)]^-$ ions. Hydrogen bonds (for indication cf. Supporting Information, Table S1b and Figure S1b) are drawn as dotted lines. (b) Cs−O interactions of a single Cs^+ ion with focus on the concurrent Cs-bonding to O1, O3, and O5 which coordinate also to V1 (Symmetry operations: $^{II} = -x, y + 1/2, -z + 1/2$; $^{III} = -x, -y, -z$; $^{IV} = x + 1/2, -y + 1/2, z + 1/2$).

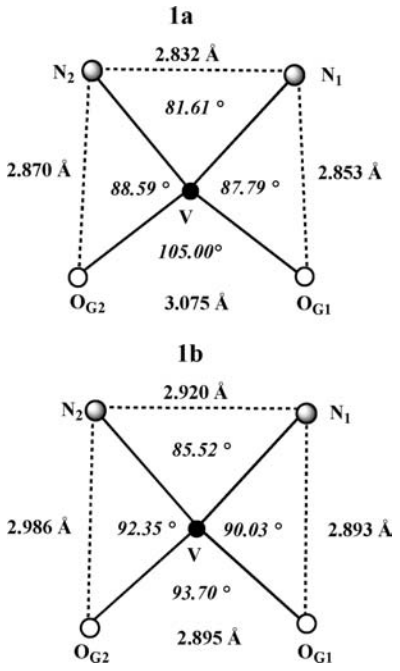

Figure 6. In-plane distances and angles (L−V−L′ angles and L···L′ site lengths) of the $VN_1N_2O_{G1}O_{G2}$ units in **1a** and **1b**.

The influence of Li−O bonding as well as H-bonding on the structural features of the complex anion in **1a** (cf. the pattern of V−L bond distances and the O3−V−O7 angles in Table 2) is apparently much weaker than the countercation influence on the VN_2O_4 arrangement of the complex anions in **1b** (Figure 6). The extensive Cs−O interactions (cf. Figure 5) of the countercation in **1b** lead to a substantial modification of the coordination sphere around V^{III} on going from **1a** to **1b**.

The difference between the angle $N_1-V-N_2 = 81.61(9)°$ in **1b** and its counterpart in **1a** ($N_1-V-N_2 = 85.5(1)°$) is coupled to a much larger variation of the $O_{G1}-V-O_{G2}$ angles where a shrinking by 11.3° takes place on going from **1a** ($O_{G1}-V-O_{G2} = 105.00(9)°$) to **1b** ($O_{G1}-V-O_{G2} = 93.7(1)°$, cf. Figure 6). This drastic reduction is certainly a consequence of the Cs−O_G interactions in **1b** where both O_{G1} (Cs−O1 = 3.082(2) Å, cf. Supporting Information, Table S1) as well as O_{G2} (Cs−O5 = 3.247(3) Å) are in direct contact with the countercation (cf. Figure 5b).

3.2. VIS/NIR- and Raman Spectra of 1a and 1b Compared to Appropriate Solution Spectra. The spectra of six- and seven-coordinate V^{III}-aminopolycarboxylato have recently been analyzed[2] based on a detailed Angular Overlap Model (AOM) analysis with the goal to establish a firm basis for differentiation between CN 6 and CN 7 V^{III} complexes.

Six-coordinate complexes with a low symmetry ligand field (C_1) usually give rise to spectra with two or three resolved VIS-bands at >14 kK (≈ 700 nm) nm which belong to transitions from the $^3A_1(^3T_{1g})$ ground state into the $^3T_{2g}(^3F)$ and $^3T_{1g}(^3P)$ excited states.[2a] The spectra of the solids **1a**, **1b** and the aqueous solution of $[V(eddadp)]^-$ shown in Figure 7 show these typical features of six-coordinate V^{III} complexes. Both the solid state spectra show additional weak absorptions at the low energy branch of band **II** at transition energies between 12 and 10 kK (800−1000 nm, omitted in Figure 7) where the spin forbidden singlet transitions of the V^{III} d^2 system appear.[28] The transition energies of bands **I** and **II** in the spectra of Figure 7 are very similar to those shown by $[V(H_2O)_6]^{3+}$ in aqueous solution, where **I** = 25.1 kK (398 nm) and **II** = 17.0 kK (588 nm).[29]

The CN increase from six to seven leads to two subtle changes in spectra of V^{III} complexes:

(i) There is a remarkable decrease of the energy for the lowest component of $^3T_{2g}(^3F)$ leading to a band shift to longer wavelengths into the region between 700 and 900 nm. This band was suggested as an indicator for CN 7 for V^{III} complexes,[9,10]

(ii) The energy of the two higher ground state split levels (from parent $^3T_{1g}$) is increased to such an extent that the resulting transitions $^3A_{(1)} \rightarrow A_{(2)}$, $^3A_{(3)}$ appear now in the NIR region. These transitions have a broad non-symmetrical shape with a maximum around 9.5 kK (1050 nm) in the spectra of the CN 7 complexes.[2] The latter band was suggested as an unambiguous test for CN 7 in V^{III} aminocarboxylato complexes.[2b] As one can see in Figure 7, both absorptions typical for CN 7 do not occur in the V^{III}-eddadp spectra recorded in this work.

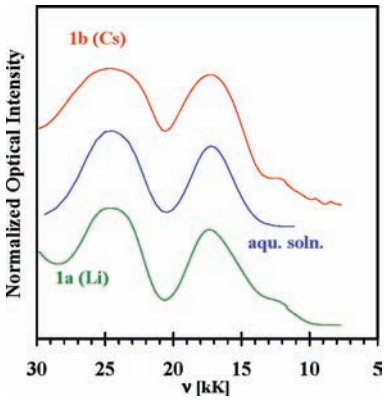

Figure 7. Comparison of the solid state VIS/NIR-spectra of **1b** and **1a** with a solution spectrum of $[V(eddadp)]^-$ in water (pH 5.0). Absorption maxima are as follows: **I** = 24.8 kK (403 nm) and **II** 17.3 kK (578 nm) for **1**b; **I** = 24.7 kK (405 nm) and **II** 17.4 kK (575 nm) for **2** (aqueous solution); **I** = 24.6 kK (407 nm) and **II** 17.2 kK (581 nm) for **1a**.

Despite the close match between the three spectra in Figure 7, a somewhat greater similarity between the spectrum of **1a** and the solution spectrum is noted. Both bands in the spectrum of **1b** are broader than their analogues in the spectra of **1a** and the solution which is especially true for the band at higher energies centered at 25 kK (400 nm). These observations indicate that CN 7 species of the type $[V(eddadp)(H_2O)]^-$ are not detectable. If they exist, their concentration must be much smaller than that of the CN 6 $[V(eddadp)]^-$ species.

(28) (a) Hush, N. S.; Hobbs, R. J. M. *Prog. Inorg. Chem.* **1968**, *10*, 284–297. (b) Tregenna-Piggott, P. L. W.; Best, S. P.; Güdel, H. U.; Weihe, H.; Wilson, C. C. *J. Solid. State Chem.* **1999**, *145*, 460. (c) Johnson, D. A.; Nelson, P. G. *Inorg. Chem.* **1999**, *38*, 4949.

(29) Meier, R.; Boddin, M.; Mitzenheim, S.; Kanamori, K. Solution Properties of Vanadium(III) with Regard to Biological Systems. In *Metal Ions in Biological Systems*; Sigel, H., Sigel, A., Eds.; M. Dekker: New York, 1995; Vol. 31, Chapter 2.

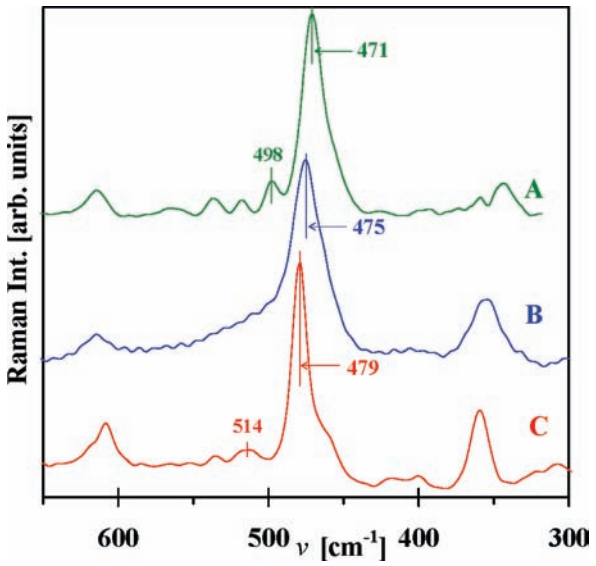

Figure 8. Comparison of the solid state Raman spectra of **1a** (**A**) and **1b** (**C**) with a solution spectrum of $[V(eddap)]^-$ in water at pH 4.5 (**B**).

The solid state Raman spectra of **1a** and **1b** are compared with a solution Raman spectrum of $[V(eddadp)]^-$ in Figure 8. As outlined before by Kanamori et al.[30] in a study of six- and seven-coordinate salts of Fe^{III}-edta and in our study of *twist-boat* and *half-chair* isomers of Fe^{III}-tmdta,[36] a valuable range for extracting information on the metal-donor atom valence vibrations as well as skeletal vibrations of the coordination cage is the 600−300 cm^{-1} region. The most intense band in all three spectra shown in Figure 8 is located in the 480−470 cm^{-1} range: at 479 cm^{-1} for **1b**, at 475 cm^{-1} for the aqueous solution and at 471 cm^{-1} for **1a**. This band can be unequivocally assigned to the twist motion of the central diamine chelate ring[36] as shown by a density functional theory (DFT) supported band assignment for the *twist-boat* form of $[Fe(tmdta)]^-$ that shows a similar arrangement of diamine chelate ring in comparison to those in the structures of **1a** and **1b**. This band is the most intense one not only in the 600−300 cm^{-1} interval of the Raman spectra of the current study but also in all Raman spectra of M^{II}-edta and M^{III}-edta complexes measured so far.[30,37] The same observation is made in Raman spectra of $[M(tmdta)]^{2-}$ and $[M(tmdta)]^-$ complexes, provided their central diamine ring is present in the *twist-boat* conformation.[30,38]

In addition to the assignment of the twist motion of the central diamine ring, Figure 8 shows the assignment of one additional band in both the spectra of **1a** (498 cm^{-1}) and **1b** (514 cm^{-1}) as well which appear both at somewhat higher energy than the former transition. In this particular wavenumber range, the ν_{as} and ν_s vibrations of the (Fe−N) bonds have been found and assigned in the case of the *twist-boat* form of $[Fe(tmdta)]^-$.[36] The difference in energy between these bands is usually quite small and not resolved in the experimental spectra. Thus, we believe it as reasonable to assign the bands at 498 cm^{-1} in the spectrum of **1a** and the one at 514 cm^{-1} in the spectrum of **1b** to the ν_{as} and ν_s vibrations of the (V−N) bonds. This conclusion is supported by the fact (cf. Table 2) that average (V−N) distance in **1a** (2.17 Å) is 0.02 Å longer than the one in **1b** (2.15 Å). A comparison of the shape of the higher-energy sites in both the solid state spectra with the spectrum recorded in aqueous solution reveals that no resolved bands are encountered in solution and only broadened shape extends from 480 to 550 cm^{-1}.

These observations do not allow or enable us to draw any definitive conclusions concerning the fraction of seven-coordinate $[V(eddadp)(H_2O)]^-$ present in aqueous solutions. Most reasonably and in agreement with results obtained during the VIS/NIR-measurements, the amounts of the CN 7 $[V(eddadp)(H_2O)]^-$ complex in these solutions is small. If significant amounts of a $[M(L)(H_2O)]$ complex would have been formed from the [M(L)] species upon dissolution in water, some extra Raman signals are expected to show up as found upon dissolution of the six-coordinate salt $Li[Fe(edta)]\cdot 3H_2O$ in water where the CN 7 species $[Fe(edta)(H_2O)]^-$ is formed.[23,30]

4. Discussion

As mentioned in the Introduction, there is a high preference for V^{III} to adopt CN 7 in edta-type complexes. These complexes are usually very stable and exceed the solution stabilities of CN 6 V^{III} complexes with analogous ligands by many orders of magnitude.[1] The amount of energy required to force a six-membered ring fragment like the trimethylenediamine ring to a N−V−N′ angle of ≈75° at a V−N distance of 2.5 Å is too large such that only CN 6 salts of $[V(tmdta)]^-$ can be isolated in the solid state.[9,31] In the case of eddadp as a ligand, the situation seems to be different, and we had to learn from the structural study of $Na[Ti(eddadp)(H_2O)]\cdot 6H_2O$[17] that a CN 7 species with eddadp as a ligand can be formed as shown in Scheme 1 by water addition to a CN 6 complex and a intramolecular rearrangement from a *trans*-O_5 geometrical isomer (cf. Chart 2) into the *trans*-O_6 form. The rearrangement places both the six-membered rings into out-of-plane positions where N−M−O bite angles of 82.6° and 83.7° are formed in the β-alaninate R rings of the CN 7 form of Ti^{III}-eddadp. The movement of the chelate rings in the model (cf. Scheme 1) is thought to be connected with a $\Lambda \rightleftharpoons \Delta$ enantiomerization of the entire complex molecule along a pseudorotational pathway (indicated by arrows in Scheme 1).

The bite angles in the three in-plane five-membered rings are 73.1° for the E ring and 71.6° and 72.5° for both the G rings. The coordination polyhedron formed is clearly a distorted pentagonal bipyramid. From a geometrical point of view no other type of CN 7 polyhedron[32] seems to be possible with eddadp as a ligand as trials using Dreiding models have shown.

(30) Kanamori, K.; Dohniwa, H.; Ukita, N.; Kanesaka, I.; Kawai, K. *Bull. Chem. Soc. Jpn.* **1990**, *63*, 1447.
(31) Boddin, M. Ph.D. Dissertation, University of Leipzig, Leipzig, Germany, 1996.
(32) Hoffmann, R.; Beier, B. F.; Mutterties, E. L.; Rossi, A. R. *Inorg. Chem.* **1977**, *16*, 511.
(33) (a) Lind, M. D.; Hamor, M. J.; Hamor, T. A.; Hoard, J. L. *Inorg. Chem.* **1964**, *3*, 34. (b) Solans, X.; Font-Altaba, M.; Garcia-Oricain, J. *Acta Crystallogr.* **1984**, *C40*, 635. (c) Solans, X.; Font-Altaba, M.; Garcia-Oricain, J. *Acta Crystallogr.* **1985**, *C41*, 525.
(34) Mitzenheim, S. Ph.D. Dissertation, University of Leipzig, Leipzig, Germany, 1997.
(35) Shannon, R. D. *Acta Crystallogr.* **1976**, *A32*, 751.
(36) Meier, R.; Maigut, J.; Kallies, B.; Lehnert, N.; Paulat, F.; Heinemann, F. W.; Zahn, G.; Feth, M. P.; Krautscheid, H.; van Eldik, R. *Chem. Commun.* **2007**, 3960.
(37) (a) Krishnan, K.; Plane, R. A. *J. Am. Chem. Soc.* **1968**, *90*, 3195. (b) Kanamori, K.; Kawai, K. *Inorg. Chem.* **1986**, *25*, 3711. (c) Meier, R.; Feth, M. P. unpublished results.
(38) Meier, R.; Lehnert, N.; Feth, M. P. unpublished results.

Scheme 1. CN 6 + H_2O ⇌ CN 7 Equilibrium in Aqueous Solutions of V^{III}-eddadp[a]

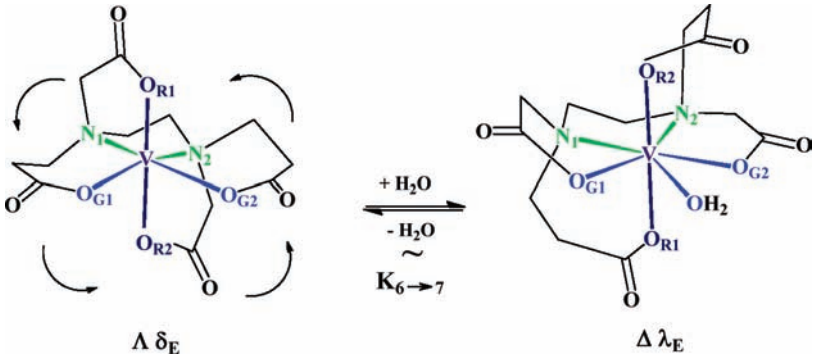

[a] The formation of the CN 7 species $[V(eddadp)(H_2O)]^-$ is accompanied by intramolecular rearrangements during which the six-membered propionate rings become R rings while the formerly axially positioned five-membered glycinate rings become G rings. The movement of the chelate rings in the model above is thought to be connected with a Λ ⇌ Δ enantiomerization of the entire complex molecule.

We[1] and others[18,24] have noted that in solid salts of the CN 7 anion $[V(edta)(H_2O)]^-$ the adoption of a PB polytope is circumvented. The latter coordination polyhedron is highly preferred in CN 7 complexes of Fe^{III}-edta[23,33] and tolerated by Ti^{III}-edta.[19] In judging the type of polytopes that can be adopted by V^{III} in any coordination polyhedron, one must consider that the electronic ground state of this d^2 ion is modified by a Jahn–Teller distortion. This means that the three degenerate t_{2g} orbitals in, for example, octahedral V^{III} complexes, split into two lower lying orbitals and one energetically higher lying metal orbital. The unpaired metal electrons are placed into both the orbitals which are lower in energy. This split is apparently partially lifted by the incursion of π electron density from the ligand donor atoms with orbitals of suitable symmetry. Such an event leads to a severe decrease in the thermodynamic stability of the appropriate V^{III} complexes.[1] Similar circumstances are obviously encountered if $[V(eddadp)]^-$ forms a CN 7 species by addition of a water molecule because only a PB polytope is expected to be formed. In such a coordination geometry, both V^{III} electrons would have to be placed in the metal d_{xz} and d_{yz} orbitals and both axially coordinating oxygens would be engaged into $O_R \rightarrow V^{III}$ π-donation into these orbitals.[32] In the case of the d^1 ion Ti^{III}, which is also subject to Jahn–Teller distortions, only one metal electron needs to be housed in both these orbitals. This can apparently resist the π influence from the oxygen donors by electrostatic repulsion which becomes evident by the elongation of one of the Ti–O_R bonds (Ti–O_{R1} = 2.064(2) Å vs Ti–O_{R2} = 2.022(2) Å; $\Delta_{R1\text{-}R2}$ = 0.042 Å). The latter bond is significantly shorter than the analogous V–O_G bonds (V–O_{Gav} = 2.09(1) Å) by 0.07 Å which should be driven by a larger amount of π bonding in the Ti–O_R bonds as compared to the Ti–O_G bonds.

Conclusions

No measurable amounts of a CN 7 species of the type $[V(eddadp)(H_2O)]^-$ could be found in aqueous solutions of V^{III}-eddadp. Also, seven-coordinate complex anions were not found in the two new salt structures that were characterized in the present study. This marks a pronounced difference with the case of the CN 7 salt $Na[Ti(eddadp)(H_2O)]\cdot 6H_2O$. The greater relative reluctance of V^{III} to form a CN 7 eddadp complex appears to stem from enhanced ligand–metal π–d electron repulsion. We cannot, however, rule out with these data the existence of a very small fraction of CN 7 aquated V^{III}-eddadp which is forced to form by the large excess of water in, for example, a millimolar complex solution. This suspicion is based on preliminary observations of the equilibrium constant for the formation of $[V(eddadp)(OH)]^{2-}$. This constant can be expressed by a pK_a value of ≈ 8[34] which is more than an order of magnitude smaller than pK_a = 9.25 for the formation of $[V(edta)(OH)]^{2-}$ from $[V(edta)(H_2O)]^-$.[1] The latter is a CN 7 species where the presence of coordinated water for deprotonation has been verified.[1,10] Our current activities are focused on the further elucidation of the interaction between electronic effects and structural preferences, and the different reaction pathways that emerge from these differences.

Acknowledgment. R.M. acknowledges financial support from the German Research Foundation (Project Me1148 7-1) and the Alexander von Humboldt Foundation (Feodor Lynen Program).

Supporting Information Available: Details of anion–cation interactions and hydrogen bonding of the complex anions in structures **1a** and **1b** are presented in Figures S1 and S2 and Tables S1 and S2, respectively. This material is available free of charge via the Internet at http://pubs.acs.org.